Advances in Computational Mathematics (2024) 50:24
https://doi.org/10.1007/s10444-024-10123-w

Robust space-time finite element methods for parabolic distributed optimal control problems with energy regularization

Ulrich Langer[1] · Olaf Steinbach[2] · Huidong Yang[3]

Received: 2 January 2023 / Accepted: 7 March 2024 / Published online: 10 April 2024

Abstract

As in our previous work (*SINUM* 59(2):660–674, 2021) we consider space-time tracking optimal control problems for linear parabolic initial boundary value problems that are given in the space-time cylinder $Q = \Omega \times (0,T)$, and that are controlled by the right-hand side z_ϱ from the Bochner space $L^2(0,T;H^{-1}(\Omega))$. So it is natural to replace the usual $L^2(Q)$ norm regularization by the energy regularization in the $L^2(0,T;H^{-1}(\Omega))$ norm. We derive new a priori estimates for the error $\|\widetilde{u}_{\varrho h} - \overline{u}\|_{L^2(Q)}$ between the computed state $\widetilde{u}_{\varrho h}$ and the desired state $\overline{u}$ in terms of the regularization parameter ϱ and the space-time finite element mesh size h, and depending on the regularity of the desired state $\overline{u}$. These new estimates lead to the optimal choice $\varrho = h^2$. The approximate state $\widetilde{u}_{\varrho h}$ is computed by means of a space-time finite element method using piecewise linear and continuous basis functions on completely unstructured simplicial meshes for Q. The theoretical results are quantitatively illustrated by a series of numerical examples in two and three space dimensions. We also provide performance studies for different solvers.

Communicated by: Stefan Volkwein

✉ Olaf Steinbach
o.steinbach@tugraz.at

Ulrich Langer
ulanger@numa.uni-linz.ac.at

Huidong Yang
huidong.yang@univie.ac.at

[1] Institute of Numerical Mathematics, Johannes Kepler University Linz, Altenberger Straße 69, 4040 Linz, Austria

[2] Institut für Angewandte Mathematik, Technische Universität Graz, Steyrergasse 30, 8010 Graz, Austria

[3] Computational Science Center, Universität Wien, Oskar–Morgenstern–Platz 1, 1090 Wien, Austria

Keywords Parabolic optimal control problems · Energy regularization · Space-time finite element methods · Error estimates · Solvers

Mathematics Subject Classification (2010) 49J20 · 49M05 · 35K20 · 65F08 · 65M60 · 65M15

1 Introduction

As in [20], we consider the minimization of the space-time tracking cost functional

$$\mathcal{J}(u_\varrho, z_\varrho) = \frac{1}{2}\int_0^T \int_\Omega [u_\varrho(x,t) - \overline{u}(x,t)]^2\, dx\, dt + \frac{1}{2}\,\varrho\, \|z_\varrho\|^2_{L^2(0,T;H^{-1}(\Omega))} \tag{1.1}$$

with respect to the state u_ϱ and the control z_ϱ subject to the model parabolic initial boundary value problem

$$\left.\begin{aligned} \partial_t u_\varrho(x,t) - \Delta_x u_\varrho(x,t) &= z_\varrho(x,t) && \text{for } (x,t) \in Q := \Omega \times (0,T),\\ u_\varrho(x,t) &= 0 && \text{for } (x,t) \in \Sigma := \partial\Omega \times (0,T),\\ u_\varrho(x,0) &= 0 && \text{for } x \in \overline{\Sigma}_0 := \overline{\Omega} \times \{0\}, \end{aligned}\right\} \tag{1.2}$$

where $\overline{u} \in L^2(Q)$ is the given desired state (target), ∂_t denotes the partial time derivative, Δ_x is the spatial Laplace operator, $\Omega \subset \mathbb{R}^n$, $n = 1, 2, 3$, is the spatial domain that is assumed to be bounded and Lipschitz, $T > 0$ is a given time horizon, and $\varrho > 0$ is a suitably chosen regularization parameter. The standard setting of such kind of optimal control problems uses the regularization in $L^2(Q)$ instead of $L^2(0, T; H^{-1}(\Omega))$; see, e.g., the books [5, 16, 35], and the references given therein. The energy regularization, as the regularization in $L^2(0, T; H^{-1}(\Omega))$ is also called, permits controls z_ϱ from the space $L^2(0, T; H^{-1}(\Omega))$ that is larger than $L^2(Q)$, and admits more concentrated controls. Such kinds of controls that are concentrated around hypersurfaces play an important role in electromagnetics in form of thinly wound coils and magnets. Moreover, the space $L^2(0, T; H^{-1}(\Omega))$ is the natural space for the source term in the variational formulation of the initial boundary value problem (1.2), at least, in the Hilbert space setting; see, e.g., [23] or [36] for solvability results. In the literature, there are other regularization techniques aiming at specific properties of the control such as sparsity and directional sparsity. We refer the reader to the recent survey article [8] where a comprehensive overview of the literature on this topic is given.

There are not so many papers investigating parabolic optimal control problems with energy regularization and using space-time methods for their numerical solution. We would like to mention the important contribution [15] to this topic, where similar parabolic optimal control problems like (1.1)–(1.2) were solved by means of a tensor-product wavelet approach. There are many contributions to different space-time approaches for the numerical solution of distributed parabolic optimal control problems with the standard L^2 regularization, e.g., [14] for an early paper, and the very recent papers [21] (unstructured space-time FEM on simplicial meshes), [19]

(unstructured stabilized space-time FEM on simplicial meshes), [11, 13] (first-order system least squares (FOSLS)), and [3] (tensor-product FEM). All of these papers consider the case of a fixed, positive regularization (cost) parameter ϱ that is not related to the mesh, and they provide discretization error estimates in different norms for fixed ϱ.

Since the state equation (1.2) in its variational form has a unique solution $u_\varrho \in X := \{u \in Y := L^2(0,T;H_0^1(\Omega)) : \partial_t u \in Y^*,\ u = 0 \text{ on } \Sigma_0\}$, for every given right-hand side $z_\varrho \in Y^* := L^2(0,T;H^{-1}(\Omega))$, the corresponding optimal control problem (1.1)–(1.2) also has a unique solution $(u_\varrho, z_\varrho) \in X \times Y^*$ that can be computed by solving the first-order optimality system or the reduced first-order optimality system where the control is eliminated by the gradient equation. The unique solvability of the state equation can also be shown by the Banach–Nečas–Babuška theorem as it was done in [31]. This theorem can also be used to show well-posedness of the reduced first-order optimality system as it was done in [20]. Now the optimal control problem (1.1)–(1.2) can be approximately solved by discretizing the reduced optimality system. Following [20], we discretize the reduced optimality system by means of a real space-time finite element method working on fully unstructured, but shape regular simplicial space-time meshes into which the space-time cylinder Q is decomposed. In [20], the authors showed a discrete inf-sup condition for the bilinear form arising from the variational formulation of the reduced optimality system. Once a discrete inf-sup condition is proven, one can easily derive the corresponding estimates for the finite element discretization error $u_\varrho - \widetilde{u}_{\varrho h}$ and $p_\varrho - \widetilde{p}_{\varrho h}$ in the corresponding norms, where $\widetilde{u}_{\varrho h}$ and $\widetilde{p}_{\varrho h}$ are the finite element solutions to the reduced first-order optimality system approximating the state u_ϱ and the co-state (adjoint) p_ϱ, respectively.

In this paper, we are investigating the error between the computed finite element solution $\widetilde{u}_{\varrho h}$ and the desired state $\overline{u}$, where we use continuous, piecewise linear finite element basis functions. This error is obviously of primary interest since one wants to know how well $\widetilde{u}_{\varrho h}$ approximates $\overline{u}$ in advance. More precisely, we derive estimates for the $L^2(Q)$ norm of this error in terms of ϱ and h, and depending on the smoothness of the target $\overline{u}$ that is assumed to belong to $H^s(Q)$ for some $s \in (0,2]$. In particular, we admit discontinuous targets that are important in many practical applications. These estimates lead to the optimal choice $\varrho = h^2$ in all cases. For elliptic optimal control problems with energy regularization, i.e., in $H^{-1}(\Omega)$, error estimates for $\|\overline{u} - u_\varrho\|_{L^2(\Omega)}$ and $\|\overline{u} - \widetilde{u}_{\varrho h}\|_{L^2(\Omega)}$ were recently derived in [26] and [22], respectively. It is interesting that, in the elliptic case, u_ϱ solves the singularly perturbed reaction-diffusion equation $-\varrho\Delta u_\varrho + u_\varrho = \overline{u}$ in Ω with homogeneous Dirichlet conditions on the boundary $\partial\Omega$, also known as differential filter in fluid mechanics [17], whereas, in the parabolic case, u_ϱ solves a similar singularly perturbed problem, but with a more complicated space-time operator of the form $B^*A^{-1}B$ replacing $-\Delta$, where $B : X \to Y^*$ is nothing but the state (parabolic) operator, and $A : Y \to Y^*$ represents the spatial Laplacian $-\Delta_x$; see Sections 2 and 3 for a more detailed discussion.

The remainder of this paper is organized as follows: Section 2 deals with the formulation of an abstract optimal control problem, and the corresponding error estimates between the desired state and the discrete state based on the exact state Schur complement equation. In Section 3, we consider a model parabolic distributed optimal control problem with energy regularization, and derive estimates for the $L^2(Q)$ error between

the desired state $\overline{u}$ and the finally computed state $\widetilde{u}_{\varrho h}$ from the perturbed state Schur complement equation for the coupled optimality system. Several numerical tests in two and three space dimensions are presented in Section 4. Here we discuss not only the quantitative convergence behavior of the $L^2(Q)$ error between the desired state $\overline{u}$ and its computed finite element approximation $\widetilde{u}_{\varrho h}$ for several benchmark problems with different features, but we also make convergence studies of the solvers that we have used in our numerical experiments. Finally, some conclusions are drawn in Section 5, and we also discuss some future research topics.

2 Abstract optimal control problems

Let $X \subset H \subset X^*$ and $Y \subset H \subset Y^*$ be Gelfand triples of Hilbert spaces, where X^*, Y^* are the duals of X, Y with respect to H, with $\langle z, v\rangle_H = \langle z, v\rangle_{Y^*\times Y}$ being the dual pairing for $z \in Y^*$, $v \in Y$. Let $A : Y \to Y^*$ and $B : X \to Y^*$ be bounded linear operators, i.e.,

$$\|Av\|_{Y^*} \le c_2^A \|v\|_Y \quad \forall v \in Y, \quad \|Bu\|_{Y^*} \le c_2^B \|u\|_X \quad \forall u \in X. \tag{2.1}$$

We assume that A is self-adjoint and elliptic in Y, and that B satisfies an inf-sup condition, i.e., there exist positive constants c_1^A and c_1^B such that

$$\langle Av, v\rangle_H \ge c_1^A \|v\|_Y^2 \quad \forall v \in Y, \quad \sup_{0\neq v\in Y} \frac{\langle Bu, v\rangle_H}{\|v\|_Y} \ge c_1^B \|u\|_X \quad \forall u \in X. \tag{2.2}$$

In addition, we assume that the dual to B operator $B^* : Y \to X^*$ is injective. Then, due to Lax–Milgram's and Banach–Nečas–Babuška's theorems (see, e.g., [10]), $A : Y \to Y^*$ and $B : X \to Y^*$ are isomorphisms. Therefore,

$$\|z\|_{Y^*} = \sqrt{\langle A^{-1}z, z\rangle_H} \quad \text{for } z \in Y^* \tag{2.3}$$

defines a norm in Y^* that is equivalent to the standard supremum norm.

We now consider the abstract minimization problem to find the minimizer $(u_\varrho, z_\varrho) \in X \times Y^*$ of the functional

$$\mathcal{J}(u_\varrho, z_\varrho) = \frac{1}{2}\|u_\varrho - \overline{u}\|_H^2 + \frac{1}{2}\varrho \|z_\varrho\|_{Y^*}^2 \quad \text{subject to } Bu_\varrho = z_\varrho, \tag{2.4}$$

when $\overline{u} \in H$ is given, and $\varrho \in \mathbb{R}_+$ is some regularization parameter. For the time being, our particular interest is focused on the behavior of $\|u_\varrho - \overline{u}\|_H$ as $\varrho \to 0$. The minimizer (u_ϱ, z_ϱ) of (2.4) is determined as the unique solution of the optimality system, see, e.g., [20],

$$Bu_\varrho = z_\varrho, \qquad B^* p_\varrho = u_\varrho - \overline{u}, \qquad p_\varrho + \varrho A^{-1} z_\varrho = 0. \tag{2.5}$$

Eliminating the control $z_\varrho \in Y^*$ and the adjoint variable $p_\varrho \in Y$ results in the operator equation to find $u_\varrho \in X$ such that

$$\varrho B^* A^{-1} B u_\varrho + u_\varrho = \overline{u} \quad \text{in } X^*. \tag{2.6}$$

Let us introduce the operator $S := B^* A^{-1} B : X \to X^*$, for which we have the following result:

Lemma 1 *There hold the inequalities*

$$\langle Su, u\rangle_H \geq c_1^S \, \|u\|_X^2 \quad \text{and} \quad \|Su\|_{X^*} \leq c_2^S \, \|u\|_X \quad \text{for all } u \in X$$

with constants

$$c_1^S = c_1^A \left(\frac{c_1^B}{c_2^A} \right)^2 \quad \text{and} \quad c_2^S = \frac{[c_2^B]^2}{c_1^A} \, .$$

Proof For arbitrary, but fixed $u \in X$, we define $\overline{p} = A^{-1} B u$ to obtain

$$\langle Su, u\rangle_H = \langle A^{-1} B u, Bu\rangle_H = \langle A\overline{p}, \overline{p}\rangle_H \geq c_1^A \, \|\overline{p}\|_Y^2 \, .$$

From the inf-sup condition (2.2) we further conclude

$$c_1^B \, \|u\|_X \leq \sup_{0 \neq v \in Y} \frac{\langle Bu, v\rangle_H}{\|v\|_Y} = \sup_{0 \neq v \in Y} \frac{\langle A\overline{p}, v\rangle_H}{\|v\|_Y} \leq \|A\overline{p}\|_{Y^*} \leq c_2^A \, \|\overline{p}\|_Y .$$

This gives

$$\langle Su, u\rangle_H \geq c_1^A \, \|\overline{p}\|_Y^2 \geq c_1^A \left(\frac{c_1^B}{c_2^A} \right)^2 \|u\|_X^2 = c_1^S \, \|u\|_X^2 .$$

To prove the second estimate, we consider

$$c_1^A \, \|\overline{p}\|_Y^2 \leq \langle A\overline{p}, \overline{p}\rangle_H = \langle Bu, \overline{p}\rangle_H \leq \|Bu\|_{Y^*} \|\overline{p}\|_Y \leq c_2^B \, \|u\|_X \|\overline{p}\|_Y ,$$

i.e.,

$$\|\overline{p}\|_Y \leq \frac{c_2^B}{c_1^A} \, \|u\|_X \, .$$

With this we finally obtain

$$\begin{aligned} \|Su\|_{X^*} &= \sup_{0 \neq v \in X} \frac{\langle Su, v\rangle_H}{\|v\|_X} = \sup_{0 \neq v \in X} \frac{\langle A^{-1} Bu, Bv\rangle_H}{\|v\|_X} \\ &= \sup_{0 \neq v \in X} \frac{\langle \overline{p}, Bv\rangle_H}{\|v\|_X} \leq \sup_{0 \neq v \in X} \frac{\|\overline{p}\|_Y \|Bv\|_{Y^*}}{\|v\|_X} \\ &\leq c_2^B \, \|\overline{p}\|_Y \leq \frac{[c_2^B]^2}{c_1^A} \, \|u\|_X = c_2^S \, \|u\|_X \, . \end{aligned}$$

□

As a consequence of Lemma 1 we also have

$$\langle Su, u\rangle_H \leq \|Su\|_{X^*}\|u\|_X \leq c_2^S \|u\|_X^2,$$

i.e.,

$$\|u\|_S^2 := \langle Su, u\rangle_H = \langle A^{-1}Bu, Bu\rangle_H$$

defines an equivalent norm in X satisfying the norm equivalence inequalities

$$c_1^S \|u\|_X^2 \leq \|u\|_S^2 \leq c_2^S \|u\|_X^2 \quad \text{for all } u \in X. \tag{2.7}$$

Now we consider the abstract operator equation to find $u_\varrho \in X$ such that

$$\varrho S u_\varrho + u_\varrho = \overline{u} \quad \text{in } X^*, \tag{2.8}$$

and its equivalent variational formulation

$$\varrho\, \langle Su_\varrho, v\rangle_H + \langle u_\varrho, v\rangle_H = \langle \overline{u}, v\rangle_H \quad \text{for all } v \in X. \tag{2.9}$$

Since S induces an equivalent norm in X, unique solvability of (2.9) follows.

Lemma 2 *For the unique solution $u_\varrho \in X$ of the variational formulation (2.9), there hold the estimates*

$$\|u_\varrho\|_H \leq \|\overline{u}\|_H \quad \text{and} \quad \varrho\, \|u_\varrho\|_S^2 \leq \|\overline{u}\|_H^2. \tag{2.10}$$

Proof For the particular choice $v = u_\varrho$ within the variational formulation (2.9), we obtain

$$\varrho\, \|u_\varrho\|_S^2 + \|u_\varrho\|_H^2 = \varrho\, \langle Su_\varrho, u_\varrho\rangle_H + \langle u_\varrho, u_\varrho\rangle_H = \langle \overline{u}, u_\varrho\rangle_H \leq \|\overline{u}\|_H \|u_\varrho\|_H,$$

from which we conclude

$$\|u_\varrho\|_H \leq \|\overline{u}\|_H$$

as well as

$$\varrho\, \|u_\varrho\|_S^2 \leq \|\overline{u}\|_H \|u_\varrho\|_H \leq \|\overline{u}\|_H^2.$$

□

Analogously to [26, Theorem 3.2] we can state the following estimates, which depend on the regularity of the given target $\overline{u} \in H$.

Lemma 3 *Let $u_\varrho \in X$ be the unique solution of the variational formulation (2.9). For $\overline{u} \in H$ there holds*

$$\|u_\varrho - \overline{u}\|_H \leq \|\overline{u}\|_H, \tag{2.11}$$

while for $\overline{u} \in X$ the following estimates hold true:

$$\|u_\varrho - \overline{u}\|_H \leq \varrho^{1/2} \|\overline{u}\|_S, \tag{2.12}$$

$$\|u_\varrho - \overline{u}\|_S \leq \|\overline{u}\|_S. \tag{2.13}$$

If in addition $S\overline{u} \in H$ is satisfied for $\overline{u} \in X$,

$$\|u_\varrho - \overline{u}\|_H \leq \varrho \, \|S\overline{u}\|_H \tag{2.14}$$

as well as

$$\|u_\varrho - \overline{u}\|_S \leq \varrho^{1/2} \, \|S\overline{u}\|_H \tag{2.15}$$

follow.

Proof From the variational formulation (2.9) and for the particular test function $v = u_\varrho$, we obtain

$$\varrho \, \|u_\varrho\|_S^2 = \varrho \, \langle Su_\varrho, u_\varrho \rangle_H = \langle \overline{u} - u_\varrho, u_\varrho \rangle_H = \langle \overline{u} - u_\varrho, \overline{u} \rangle_H - \langle \overline{u} - u_\varrho, \overline{u} - u_\varrho \rangle_H,$$

which gives

$$\varrho \, \|u_\varrho\|_S^2 + \|u_\varrho - \overline{u}\|_H^2 = \langle \overline{u} - u_\varrho, \overline{u} \rangle_H \leq \|\overline{u} - u_\varrho\|_H \|\overline{u}\|_H,$$

i.e., (2.11) follows.

When assuming $\overline{u} \in X$, we can choose $v = \overline{u} - u_\varrho \in X$ as test function in (2.9) to conclude

$$\begin{aligned} \|\overline{u} - u_\varrho\|_H^2 &= \langle \overline{u} - u_\varrho, \overline{u} - u_\varrho \rangle_H \\ &= \varrho \, \langle Su_\varrho, \overline{u} - u_\varrho \rangle_H \\ &= \varrho \, \langle S\overline{u}, \overline{u} - u_\varrho \rangle_H - \varrho \, \langle S(\overline{u} - u_\varrho), \overline{u} - u_\varrho \rangle_H, \end{aligned} \tag{2.16}$$

i.e.,

$$\varrho \, \|\overline{u} - u_\varrho\|_S^2 + \|\overline{u} - u_\varrho\|_H^2 = \varrho \, \langle S\overline{u}, \overline{u} - u_\varrho \rangle_H \leq \varrho \, \|\overline{u}\|_S \|\overline{u} - u_\varrho\|_S \, .$$

In a first step this gives (2.13),

$$\|u_\varrho - \overline{u}\|_S \leq \|\overline{u}\|_S.$$

With this we further obtain

$$\|u_\varrho - \overline{u}\|_H^2 \leq \varrho \, \|\overline{u}\|_S \|\overline{u} - u_\varrho\|_S \leq \varrho \, \|\overline{u}\|_S^2,$$

i.e., (2.12) follows.

If, for $\overline{u} \in X$, we have in addition $S\overline{u} \in H$, from the estimate (2.16), we also conclude

$$\varrho \, \|\overline{u} - u_\varrho\|_S^2 + \|\overline{u} - u_\varrho\|_H^2 = \varrho \, \langle S\overline{u}, \overline{u} - u_\varrho \rangle_H \leq \varrho \, \|S\overline{u}\|_H \|u_\varrho - \overline{u}\|_H,$$

from which (2.14) follows. Finally, the estimates

$$\varrho \, \|\overline{u} - u_\varrho\|_S^2 \leq \varrho \, \|S\overline{u}\|_H \|u_\varrho - \overline{u}\|_H \leq \varrho^2 \, \|S\overline{u}\|_H^2$$

imply (2.15). □

Based on the estimates as given in Lemma 3 and in the case of the particular application we have in mind, we can derive more general estimates which are based on interpolation arguments in a scale of Sobolev spaces. This will be discussed later in more detail.

For some conforming approximation space $X_h \subset X$, we now consider the Galerkin variational formulation of (2.9), i.e., find $u_{\varrho h} \in X_h$ such that

$$\varrho \, \langle S u_{\varrho h}, v_h \rangle_H + \langle u_{\varrho h}, v_h \rangle_H = \langle \overline{u}, v_h \rangle_H \quad \forall \, v_h \in X_h. \tag{2.17}$$

Using again standard arguments, we conclude unique solvability of (2.17), and the following Cea type a priori error estimate,

$$\| u_\varrho - u_{\varrho h} \|_H \leq \inf_{v_h \in X_h} \sqrt{\varrho \, \| u_\varrho - v_h \|_S^2 + \| u_\varrho - v_h \|_H^2}. \tag{2.18}$$

As a particular application of (2.18) we obtain, when choosing $v_h = 0$, and using (2.10),

$$\| u_\varrho - u_{\varrho h} \|_H^2 \leq \varrho \, \| u_\varrho \|_S^2 + \| u_\varrho \|_H^2 \leq 2 \, \| \overline{u} \|_H^2.$$

Now, using (2.11), we conclude the abstract error estimate

$$\| u_{\varrho h} - \overline{u} \|_H \leq \| u_\varrho - \overline{u} \|_H + \| u_\varrho - u_{\varrho h} \|_H \leq (1 + \sqrt{2}) \, \| \overline{u} \|_H. \tag{2.19}$$

when assuming $\overline{u} \in H$ only.

3 Parabolic distributed optimal control problem

The parabolic optimal control problem (1.1)–(1.2) as given in the introduction is obviously a special case of the abstract optimal control problem (2.4). Indeed, in view of the abstract setting, we have $H := L^2(Q)$, $Y := L^2(0, T; H_0^1(\Omega))$, and

$$X := \{ u \in W(0, T) : u = 0 \text{ on } \Sigma_0 \},$$

with $W(0, T) := \{ u \in Y : \partial_t u \in Y^* = L^2(0, T; H^{-1}(\Omega)) \}$. The related norms in Y, X, and Y^* are given by

$$\| v \|_Y := \| \nabla_x v \|_{L^2(Q)}, \quad \| u \|_X := \sqrt{\| u \|_Y^2 + \| \partial_t u \|_{Y^*}^2}, \quad \text{and} \quad \| \partial_t u \|_{Y^*} = \| \nabla_x w_u \|_{L^2(Q)},$$

respectively, where $w_u \in Y$ is the unique solution of the variational problem

$$\langle \nabla_x w_u, \nabla_x v \rangle_{L^2(Q)} = \langle \partial_t u, v \rangle_Q \quad \forall \, v \in Y,$$

and where $\langle \partial_t u, v \rangle_Q$ is the dual pairing for $\partial_t u \in Y^*$ and $v \in Y$. For later use, we will prove the following embedding:

Lemma 4 *For $u \in X \cap H^1(Q)$ there holds*

$$\|u\|_X \leq \max\{\sqrt{c_F}, 1\}\, \|u\|_{H^1(Q)} \tag{3.1}$$

with the constant $c_F > 0$ from the spatial Friedrichs inequality in $H_0^1(\Omega)$,

$$\int_\Omega [v(x)]^2\, dx \;\leq\; c_F \int_\Omega |\nabla_x v(x)|^2\, dx \quad \forall\, v \in H_0^1(\Omega). \tag{3.2}$$

Proof Recall that we can write

$$\|u\|_X^2 = \|\partial_t u\|_{Y^*}^2 + \|\nabla_x u\|_{L^2(Q)}^2,$$

and since $\partial_t u \in L^2(Q)$ for $u \in H^1(Q)$, we can bound $\|\partial_t u\|_{Y^*}$ as follows:

$$\|\partial_t u\|_{Y^*} = \sup_{0 \neq v \in Y} \frac{\langle \partial_t u, v\rangle_Q}{\|v\|_Y} \leq \sup_{0 \neq v \in Y} \frac{\|\partial_t u\|_{L^2(Q)} \|v\|_{L^2(Q)}}{\|\nabla_x v\|_{L^2(Q)}} \leq \sqrt{c_F}\, \|\partial_t u\|_{L^2(Q)}.$$

Here we have used the Friedrich's inequality

$$\|v\|_{L^2(Q)}^2 = \int_0^T \|v(t)\|_{L^2(\Omega)}^2\, dt \leq c_F \int_0^T \|\nabla_x v(t)\|_{L^2(\Omega)}^2\, dt = c_F\, \|\nabla_x v\|_{L^2(Q)}^2$$

that holds for all $v \in Y = L^2(0, T; H_0^1(\Omega))$ due to (3.2). Hence, the estimates

$$\|u\|_X^2 \leq c_F\, \|\partial_t u\|_{L^2(Q)}^2 + \|\nabla_x u\|_{L^2(Q)}^2 \leq \max\{c_F, 1\}\, \|u\|_{H^1(Q)}^2$$

follow. □

The variational formulation of the state equation (1.2) can now be written in the form: Find $u_Q \in X$ such that

$$\int_0^T \int_\Omega \Big[\partial_t u_Q(x,t)\, v(x,t) + \nabla_x u_Q(x,t) \cdot \nabla_x v(x,t)\Big]\, dx\, dt = \int_0^T \int_\Omega z_Q(x,t)\, v(x,t)\, dx\, dt$$

for all $v \in Y$, where the first term in the bilinear form and the right-hand side must be understood as duality pairing between Y^* and Y. This variational formulation can be rewritten as operator equation $Bu_Q = z_Q$ in $Y^* = L^2(0, T; H^{-1}(\Omega))$. The operator $B : X \to Y^*$ is therefore defined by the variational identity

$$\langle Bu, v\rangle_Q = \int_0^T \int_\Omega \Big[\partial_t u(x,t)\, v(x,t) + \nabla_x u(x,t) \cdot \nabla_x v(x,t)\Big]\, dx\, dt \tag{3.3}$$

for all $u \in X$ and $v \in Y$, while $A : Y \to Y^*$ is given as

$$\langle Aw, v\rangle_Q = \int_0^T \int_\Omega \nabla_x w(x,t) \cdot \nabla_x v(x,t)\, dx\, dt, \quad \forall\, w, v \in Y. \tag{3.4}$$

We obviously have $c_1^A = c_2^A = 1$. Following [31, 32], the operator $B : X \to Y^*$ is bounded,

$$\langle Bu, v\rangle_Q \le \sqrt{2}\, \|u\|_X \|v\|_Y \quad \forall\, u \in X,\ v \in Y,$$

and satisfies the inf-sup condition

$$\frac{1}{\sqrt{2}} \|u\|_X \le \sup_{0 \neq v \in Y} \frac{\langle Bu, v\rangle_Q}{\|v\|_Y} \quad \forall\, u \in X,$$

i.e., $c_1^B = 1$ and $c_2^B = \sqrt{2}$. Hence we obtain the statements of Lemma 1 with $c_1^S = 1$ and $c_2^S = 2$. With these definitions, the reduced first-order optimality system can be written in the weak form: Find $(u_\varrho, p_\varrho) \in X \times Y$ such that

$$\varrho^{-1} \int_0^T \int_\Omega \nabla_x p_\varrho \cdot \nabla_x q\, dx\, dt + \int_0^T \int_\Omega \Big[\partial_t u_\varrho\, q + \nabla_x u_\varrho \cdot \nabla_x q\Big]\, dx\, dt = 0,$$

$$\int_0^T \int_\Omega \Big[p_\varrho\, \partial_t v + \nabla_x p_\varrho \cdot \nabla_x v\Big]\, dx\, dt - \int_0^T \int_\Omega u_\varrho\, v\, dx\, dt = -\int_0^T \int_\Omega \overline{u}\, v\, dx\, dt,$$

for all $q \in Y$ and $v \in X$, which can now be rewritten in the equivalent operator form

$$\begin{pmatrix} \varrho^{-1} A & B \\ B^* & -I \end{pmatrix} \begin{pmatrix} p_\varrho \\ u_\varrho \end{pmatrix} = \begin{pmatrix} 0 \\ -\overline{u} \end{pmatrix} \quad \text{in} \quad Y^* \times X^*. \tag{3.5}$$

We note that the homogeneous initial condition for the state u_ϱ is incorporated in the state space X as essential condition in the same way as the homogeneous Dirichlet boundary conditions for the state and the adjoint, whereas the homogeneous end condition imposed on the adjoint p_ϱ at $t = T$ is built into the weak form of the adjoint equation as natural condition after integration by parts in time. Once (3.5) is solved, we can compute the control z_ϱ by the gradient equation $z_\varrho = -\varrho^{-1} A p_\varrho$; cf. also (2.5) and (2.6).

For the Galerkin formulation (2.17), we introduce the conforming finite element space $X_h = S_h^1(Q) \cap X \subset X$ spanned by piecewise linear and continuous basis functions which are defined with respect to some admissible decomposition of the space-time domain Q into shape regular simplicial finite elements of mesh width h; see, e.g., [7]. We note that the finite element functions from X_h vanish on $\overline{\Sigma} \cup \overline{\Sigma}_0$. Then the finite element approximation of (2.9) reads to find $u_{\varrho h} \in X_h$ such that

$$\varrho\, \langle B^* A^{-1} B u_{\varrho h}, v_h\rangle_Q + \langle u_{\varrho h}, v_h\rangle_{L^2(Q)} = \langle \overline{u}, v_h\rangle_{L^2(Q)} \tag{3.6}$$

is satisfied for all $v_h \in X_h$.

As in [24, Definition 2.1, page 10] we make use of the intermediate spaces $[X, Y]_s$ for $s \in [0, 1]$ when X is dense in Y with continuous injection; see also [34].

Theorem 1 *Assume $\overline{u} \in [X, L^2(Q)]_s \cap H^s(Q)$ for $s \in [0, 1)$ or $\overline{u} \in X \cap H^s(Q)$ for $s \in [1, 2]$. For the unique solution $u_{\varrho h} \in X_h$ of (3.6), the finite element error estimate*

$$\|u_{\varrho h} - \overline{u}\|_{L^2(Q)} \leq c\, h^s\, \|\overline{u}\|_{H^s(Q)} \tag{3.7}$$

holds provided that $\varrho = h^2$.

Proof For $\overline{u} \in L^2(Q)$, we can write the error estimate (2.19) as

$$\|u_{\varrho h} - \overline{u}\|_{L^2(Q)} \leq (1 + \sqrt{2})\, \|\overline{u}\|_{L^2(Q)}.$$

Due to $X \subset H^1(Q)$, we now assume $\overline{u} \in X \cap H^1(Q)$ for which we can write the error estimate (2.18) as

$$\begin{aligned}
\|u_\varrho - u_{\varrho h}\|^2_{L^2(Q)} &\leq \inf_{v_h \in X_h} \Big[\varrho\, \|u_\varrho - v_h\|^2_S + \|u_\varrho - v_h\|^2_{L^2(Q)} \Big] \\
&\leq 2 \Big[\varrho\, \|u_\varrho - \overline{u}\|^2_S + \|u_\varrho - \overline{u}\|^2_{L^2(Q)} + \inf_{v_h \in X_h} \Big[\varrho\, \|\overline{u} - v_h\|^2_S + \|\overline{u} - v_h\|^2_{L^2(Q)} \Big] \Big] \\
&\leq 4\, \varrho\, \|\overline{u}\|^2_S + 2 \inf_{v_h \in X_h} \Big[\varrho\, \|\overline{u} - v_h\|^2_S + \|\overline{u} - v_h\|^2_{L^2(Q)} \Big] \\
&\leq 8\, \varrho\, \|\overline{u}\|^2_X + 2 \inf_{v_h \in X_h} \Big[2\, \varrho\, \|\overline{u} - v_h\|^2_X + \|\overline{u} - v_h\|^2_{L^2(Q)} \Big] \\
&\leq 8\, \max\{c_F, 1\}\, \varrho\, \|\overline{u}\|^2_{H^1(Q)} \\
&\qquad + 2 \inf_{v_h \in X_h} \Big[2\, \max\{c_F, 1\}\, \varrho\, \|\overline{u} - v_h\|^2_{H^1(Q)} + \|\overline{u} - v_h\|^2_{L^2(Q)} \Big]
\end{aligned}$$

when using (2.13) and (2.12), the upper norm equivalence inequality in (2.7) with $c_2^S = 2$, and $\|\overline{u}\|_{H^1(Q)}$ as upper bound of $\|\overline{u}\|_X$, see (3.1). Now inserting a suitable H^1-stable quasi-interpolation $v_h = P_h \overline{u} \in X_h$ of the desired state $\overline{u} \in H^1(Q)$, e.g., Scott–Zhang's interpolation [7], we immediately obtain the estimate

$$\|u_\varrho - u_{\varrho h}\|^2_{L^2(Q)} \leq c\, [\varrho + h^2]\, \|\overline{u}\|^2_{H^1(Q)}.$$

Combining this estimate with (2.12) and choosing $\varrho = h^2$ finally gives

$$\|u_{\varrho h} - \overline{u}\|_{L^2(Q)} \leq c\, h\, \|\overline{u}\|_{H^1(Q)}.$$

Next we consider $\overline{u} \in X \cap H^2(Q)$ which guarantees $S\overline{u} \in L^2(Q)$. Similar as above, but now using (2.14) and (2.15), we then obtain the estimates

$$\begin{aligned}\|u_{\varrho h} - \overline{u}\|^2_{L^2(Q)} &\le 2\,\|u_{\varrho h} - u_\varrho\|^2_{L^2(Q)} + 2\,\|u_\varrho - \overline{u}\|^2_{L^2(Q)} \\ &\le 10\,\varrho^2\,\|S\overline{u}\|^2_{L^2(Q)} + 4\,\inf_{v_h \in X_h}\left[\varrho\,\|\overline{u} - v_h\|^2_S + \|\overline{u} - v_h\|^2_{L^2(Q)}\right] \\ &\le c\,[\varrho^2 + \varrho h^2 + h^4]\,\|\overline{u}\|_{H^2(Q)}\,.\end{aligned}$$

Here we have used the estimate

$$\|S\overline{u}\|_{L^2(Q)} \le c\,\|\overline{u}\|_{H^2(Q)}$$

that can be shown by Fourier analysis; cf. [32]. Choosing $\varrho = h^2$ yields

$$\|u_{\varrho h} - \overline{u}\|_{L^2(Q)} \le c\,h^2\,\|\overline{u}\|_{H^2(Q)}\,.$$

The general estimate for $s \in [0, 1)$ and $s \in [1, 2]$ now follows from a space interpolation argument; see, e.g., [34]. □

Corollary 1 *Let us assume that $\overline{u} \in X \cap H^s(Q)$ for some $s \in [1, 2]$. Then there holds the error estimate*

$$\|u_{\varrho h} - \overline{u}\|_X \le c\,h^{s-1}\|\overline{u}\|_{H^s(Q)}. \tag{3.8}$$

Proof Let $P_h\overline{u} \in X_h$ be again Scott–Zhang's interpolation of $\overline{u} \in H^1(Q)$. Using an inverse inequality and standard arguments we obtain

$$\begin{aligned}\|u_{\varrho h} - \overline{u}\|_X &\le \|u_{\varrho h} - \overline{u}\|_{H^1(Q)} \\ &\le \|u_{\varrho h} - P_h\overline{u}\|_{H^1(Q)} + \|P_h\overline{u} - \overline{u}\|_{H^1(Q)} \\ &\le c\,h^{-1}\,\|u_{\varrho h} - P_h\overline{u}\|_{L^2(Q)} + c\,h^{s-1}\,\|\overline{u}\|_{H^s(Q)} \\ &\le c\,h^{-1}\left[\|u_{\varrho h} - \overline{u}\|_{L^2(Q)} + \|\overline{u} - P_h\overline{u}\|_{L^2(Q)}\right] + c\,h^{s-1}\,\|\overline{u}\|_{H^s(Q)} \\ &\le c\,h^{s-1}\,\|\overline{u}\|_{H^s(Q)}\,.\end{aligned}$$

□

Since (3.6) requires, for any given $w \in X$, the evaluation of $Sw = B^*A^{-1}Bw$, we have to define a suitable computable approximation $\widetilde{S}w$. This can be done as follows. For given $w \in X$, we introduce $p_w = A^{-1}Bw \in Y$ as the unique solution of the variational formulation

$$\langle Ap_w, q\rangle_Q = \langle Bw, q\rangle_Q \quad \forall\, q \in Y.$$

Let $p_{wh} \in Y_h = S^1_h(Q) \cap Y \subset Y$ be the continuous, piecewise linear space-time finite element approximation to $p_w \in Y$, satisfying

$$\langle Ap_{wh}, q_h\rangle_Q = \langle Bw, q_h\rangle_Q \quad \forall\, q_h \in Y_h. \tag{3.9}$$

We note that the finite element functions from Y_h are vanishing on $\overline{\Sigma}$, but neither at the initial or final time. With this we define the approximate operator $\widetilde{S}w := B^* p_{wh}$ of $Sw = B^* p_w$. The boundedness of $B : X \to Y^*$ implies

$$\|\widetilde{S}w\|_{X^*} = \|B^* p_{wh}\|_{X^*} \leq c_2^B \, \|p_{wh}\|_X ,$$

while the ellipticity of $A : Y \to Y^*$ gives

$$c_1^A \, \|p_{wh}\|_Y^2 \leq \langle A p_{wh}, p_{wh} \rangle_Q = \langle B w, p_{wh} \rangle_Q \leq c_2^B \, \|w\|_X \|p_{wh}\|_Y ,$$

i.e.,

$$\|p_{wh}\|_Y \leq \frac{c_2^B}{c_1^A} \, \|w\|_X .$$

Hence, we conclude the boundedness of the approximate operator $\widetilde{S} : X \to X^*$,

$$\|\widetilde{S}w\|_{X^*} \leq c_2^{\widetilde{S}} \, \|w\|_X \quad \forall \, w \in X, \quad c_2^{\widetilde{S}} = \frac{[c_2^B]^2}{c_1^A} = 2. \tag{3.10}$$

Moreover,

$$\langle \widetilde{S}w, w \rangle_Q = \langle B^* p_{wh}, w \rangle_Q = \langle B w, p_{wh} \rangle_Q = \langle A p_{wh}, p_{wh} \rangle_Q \geq 0$$

implies that $\widetilde{S}$ is non-negative. Instead of (3.6), we now consider the perturbed variational formulation to find $\widetilde{u}_{\varrho h} \in X_h$ such that

$$\varrho \, \langle \widetilde{S} \widetilde{u}_{\varrho h}, v_h \rangle_Q + \langle \widetilde{u}_{\varrho h}, v_h \rangle_{L^2(Q)} = \langle \overline{u}, v_h \rangle_{L^2(Q)} \tag{3.11}$$

is satisfied for all $v_h \in X_h$. Unique solvability of (3.11) follows since the stiffness matrix of the non-negative operator $\widetilde{S}$ is positive semi-definite, while the mass matrix, which is related to the inner product in $L^2(Q)$, is positive definite.

Lemma 5 *Let $u_{\varrho h} \in X_h$ and $\widetilde{u}_{\varrho h} \in X_h$ be the unique solutions of the variational formulations (3.6) and (3.11), respectively. Assume $\overline{u} \in X \cap H^1(Q)$. Then, there holds the error estimate*

$$\|u_{\varrho h} - \widetilde{u}_{\varrho h}\|_{L^2(Q)} \leq c \, h \, \|\overline{u}\|_{H^1(Q)}.$$

Proof The difference of the variational formulations (3.6) and (3.11) first gives the Galerkin orthogonality

$$\varrho \, \langle S u_{\varrho h} - \widetilde{S} \widetilde{u}_{\varrho h}, v_h \rangle_Q + \langle u_{\varrho h} - \widetilde{u}_{\varrho h}, v_h \rangle_{L^2(Q)} = 0 \quad \forall \, v_h \in X_h,$$

which can be written as

$$\varrho \, \langle \widetilde{S}(\widetilde{u}_{\varrho h} - u_{\varrho h}), v_h \rangle_Q + \langle \widetilde{u}_{\varrho h} - u_{\varrho h}, v_h \rangle_{L^2(Q)} = \varrho \, \langle (S - \widetilde{S}) u_{\varrho h}, v_h \rangle_Q \quad \forall \, v_h \in X_h.$$

In particular, choosing $v_h = \widetilde{u}_{\varrho h} - u_{\varrho h} \in X_h$, using $\langle \widetilde{S} w, w \rangle_Q \geq 0$ for all $w \in X$, applying an inverse inequality in X_h, i.e., using the dual norm for $\|\partial_t v_h\|_{Y^*}$ and Friedrich's inequality (3.2), we arrive at the estimates

$$\begin{aligned}\|\widetilde{u}_{\varrho h} - u_{\varrho h}\|^2_{L^2(Q)} &\leq \varrho \, \langle (S - \widetilde{S}) u_{\varrho h}, \widetilde{u}_{\varrho h} - u_{\varrho h} \rangle_Q \\ &\leq \varrho \, \|(S - \widetilde{S}) u_{\varrho h}\|_{X^*} \|\widetilde{u}_{\varrho h} - u_{\varrho h}\|_X \\ &\leq c \, \varrho \, h^{-1} \, \|(S - \widetilde{S}) u_{\varrho h}\|_{X^*} \|\widetilde{u}_{\varrho h} - u_{\varrho h}\|_{L^2(Q)},\end{aligned}$$

i.e.,

$$\|\widetilde{u}_{\varrho h} - u_{\varrho h}\|_{L^2(Q)} \leq c \, \varrho \, h^{-1} \, \|(S - \widetilde{S}) u_{\varrho h}\|_{X^*}.$$

Since $\overline{u} \in X$, we can further estimate

$$\begin{aligned}\|\widetilde{u}_{\varrho h} - u_{\varrho h}\|_{L^2(Q)} &\leq c \, \varrho \, h^{-1} \left[\|(S - \widetilde{S})(u_{\varrho h} - \overline{u})\|_{X^*} + \|(S - \widetilde{S})\overline{u}\|_{X^*} \right] \\ &\leq c \, \varrho \, h^{-1} \left[4 \, \|u_{\varrho h} - \overline{u}\|_X + \sqrt{2} \, \|p_{\overline{u}} - p_{\overline{u}h}\|_Y \right],\end{aligned}$$

where we used the boundedness of S and $\widetilde{S}$. We note that $p_{\overline{u}} = A^{-1} B \overline{u}$, and $p_{\overline{u}h} \in Y_h$ solves (3.9) with $w = \overline{u}$. For $\overline{u} \in H^1(Q)$, we can use standard arguments as well as (3.1) to bound

$$\|p_{\overline{u}} - p_{\overline{u}h}\|_Y \leq \|p_{\overline{u}}\|_Y = \|A^{-1} B \overline{u}\|_Y \leq \frac{c_2^B}{c_1^A} \, \|\overline{u}\|_X \leq \sqrt{2} \, \max\{\sqrt{c_F}, 1\} \, \|\overline{u}\|_{H^1(Q)},$$

and using (3.8) for $s = 1$ we finally obtain, using $\varrho = h^2$,

$$\|\widetilde{u}_{\varrho h} - u_{\varrho h}\|_{L^2(Q)} \leq c \, h \, \|\overline{u}\|_{H^1(Q)}.$$

□

Theorem 2 *Assume $\overline{u} \in [X, L^2(Q)]_s \cap H^s(Q)$ for $s \in [0, 1]$, and $\varrho = h^2$. Then,*

$$\|\widetilde{u}_{\varrho h} - \overline{u}\|_{L^2(Q)} \leq c \, h^s \, \|\overline{u}\|_{H^s(Q)}. \tag{3.12}$$

Proof For $s = 1$ the assertion is an immediate consequence of Theorem 1 and Lemma 5. Now we consider (3.11) for $v_h = \widetilde{u}_{\varrho h}$,

$$\varrho \, \langle \widetilde{S} \widetilde{u}_{\varrho h}, \widetilde{u}_{\varrho h} \rangle_Q + \langle \widetilde{u}_{\varrho h} - \overline{u}, \widetilde{u}_{\varrho h} - \overline{u} \rangle_{L^2(Q)} = \langle \overline{u} - \widetilde{u}_{\varrho h}, \overline{u} \rangle_{L^2(Q)},$$

from which we immediately conclude

$$\|\widetilde{u}_{\varrho h} - \overline{u}\|_{L^2(Q)} \leq \|\overline{u}\|_{L^2(Q)}.$$

The assertion then again follows by a space interpolation argument. □

The error estimate as given in (3.12) covers in particular the case when the target is either discontinuous, or does not satisfy the required boundary or initial conditions. It remains to consider the case when the target $\overline{u}$ is smooth. As in the proof of Lemma 5, and using (3.8) for $s = 2$, we now have, recall $\varrho = h^2$,

$$\begin{aligned}\|\widetilde{u}_{\varrho h} - u_{\varrho h}\|_{L^2(Q)} &\leq c\,\varrho\,h^{-1}\left[4\,\|u_{\varrho h} - \overline{u}\|_X + \sqrt{2}\,\|p_{\overline{u}} - p_{\overline{u}h}\|_Y\right] \\ &\leq c_1\,h^2\,\|\overline{u}\|_{H^2(Q)} + c_2\,h\,\|p_{\overline{u}} - p_{\overline{u}h}\|_Y\,.\end{aligned}$$

When using the approximation result as given in [31, Theorem 3.3] we have

$$\|p_{\overline{u}} - p_{\overline{u}h}\|_Y \leq c\,h\,\|p_{\overline{u}}\|_{H^2(Q)}, \tag{3.13}$$

i.e., we obtain

$$\|\widetilde{u}_{\varrho h} - u_{\varrho h}\|_{L^2(Q)} \leq c\,h^2\left[\|\overline{u}\|_{H^2(Q)} + \|p_{\overline{u}}\|_{H^2(Q)}\right]. \tag{3.14}$$

While the error estimate (3.13) holds for any admissible decomposition of the space-time domain Q into simplicial finite elements, in addition to $\overline{u} \in X \cap H^2(Q)$, we have to assume $p_{\overline{u}} = A^{-1}B\overline{u} \in H^2(Q)$, i.e., $\overline{u} \in H^{2,3}(Q)$. This additional regularity requirement in time is due to the finite element error estimate (3.13) which does not reflect the anisotropic behavior in space and time of the norm in $Y = L^2(0,T;H_0^1(\Omega))$. However, and as already discussed in [31, Corollary 4.2], we can improve the error estimate (3.13) under additional assumptions on the underlying space-time finite element mesh. In fact, when considering as in [31, Section 4] right-angled space-time finite elements, or space-time tensor-product meshes, instead of (3.13) we obtain the error estimate

$$\|p_{\overline{u}} - p_{\overline{u}h}\|_Y \leq c\,h\,|\nabla_x p_{\overline{u}}|_{H^1(Q)}, \tag{3.15}$$

when assuming $\nabla_x p_{\overline{u}} \in H^1(Q)$ for $p_{\overline{u}} = A^{-1}B\overline{u}$, i.e., there are no second-order time derivatives yet. This is the reason to further conclude the bound

$$\|p_{\overline{u}} - p_{\overline{u}h}\|_Y \leq c\,h\,\|\overline{u}\|_{H^2(Q)},$$

and hence,

$$\|\widetilde{u}_{\varrho h} - u_{\varrho h}\|_{L^2(Q)} \leq c\,h^2\,\|\overline{u}\|_{H^2(Q)} \tag{3.16}$$

follows, when assuming $\overline{u} \in X \cap H^2(Q)$. Now, interpolating (3.12) for $s = 1$ and (3.16), we conclude

$$\|\widetilde{u}_{\varrho h} - u_{\varrho h}\|_{L^2(Q)} \leq c\,h^s\,\|\overline{u}\|_{H^s(Q)} \quad \text{for } \overline{u} \in X \cap H^s(Q),\ s \in [1,2] \tag{3.17}$$

that together with estimate (3.7) from Theorem 1 finally gives

$$\|\widetilde{u}_{\varrho h} - \overline{u}\|_{L^2(Q)} \leq c\,h^s\,\|\overline{u}\|_{H^s(Q)}. \tag{3.18}$$

While we can prove this result for some structured space-time finite element meshes only, numerical experiments indicate that (3.18) remains true for any admissible decomposition of the space-time domain into simplicial finite elements.

4 Numerical results

In the numerical experiments, we choose the spatial domain $\Omega = (0,1)^n$ with $n = 2$ (Section 4.1) and $n = 3$ (Section 4.2), and final time $T = 1$, resulting in the $n+1$-dimensional space-time cylinder $Q = (0,1)^{n+1}$. We follow the space-time finite element method on fully unstructured simplicial meshes as considered in [20] for the coupled optimality system of the parabolic distributed control problem (1.1). We mention that the refinement of the tetrahedrons ($n = 2$) is based on Bey's algorithm [4], whereas the refinement of the pentatops ($n = 3$) uses Stevenson's bisection method [33]. This finally leads to the solution of a saddle-point system that is nothing but the discrete version of (3.5): Find the nodal parameter vectors $\underline{p} \in \mathbb{R}^{M_Y}$ ($M_Y = \dim(Y_h)$) and $\underline{u} \in \mathbb{R}^{M_X}$ ($M_X = \dim(X_h)$) such that

$$\begin{pmatrix} \varrho^{-1} A_h & B_h \\ B_h^\top & -M_h \end{pmatrix} \begin{pmatrix} \underline{p} \\ \underline{u} \end{pmatrix} = \begin{pmatrix} \underline{0} \\ -\underline{f} \end{pmatrix}, \tag{4.1}$$

where the finite element matrices A_h, B_h, and M_h correspond to the bilinear forms (3.4) and (3.3), and to the $L^2(Q)$ inner product, respectively. The matrices $A_h \in \mathbb{R}^{M_Y \times M_Y}$ and $M_h \in \mathbb{R}^{M_X \times M_X}$ are symmetric and positive definite, while the matrix $B_h \in \mathbb{R}^{M_Y \times M_X}$ is in general rectangular. The load vector $\underline{f} \in \mathbb{R}^{N_X}$ is computed from the given target $\overline{u}$ as usual. We mention that the symmetric, but indefinite system (4.1) is equivalent to solving the related Schur complement system

$$\left(\varrho B_h^\top A_h^{-1} B_h + M_h \right) \underline{u} = \underline{f} \tag{4.2}$$

that corresponds to (3.11). Here, the symmetric but indefinite system (4.1) is simply solved by the ILU(0) preconditioned GMRES method; see [20]. We stop the GMRES iteration when the relative residual error of the preconditioned system is reduced by a factor 10^7. Of course, the ILU(0) preconditioner does not produce a solver of asymptotically optimal complexity; see also performance studies for Example 4.1.4 in Section 4.3. In the same subsection, we also present the theoretical foundation and numerical results for solvers that are of asymptotically almost optimal complexity with respect to both memory demand and arithmetical operations.

4.1 Two space dimensions

In the first example (Example 4.1.1), we consider the smooth target

$$\overline{u}(x,t) = \sin(\pi x_1) \sin(\pi x_2) \sin(\pi t) \tag{4.3}$$

where we can apply the error estimate (3.14). As predicted, we observe a second-order convergence with respect to the mesh size h when choosing $\varrho = h^2$; see also the experimental order of convergence (eoc) in Table 1.

As a second example (Example 4.1.2), we consider a piecewise linear continuous function $\overline{u}$ being one at the midpoint $(1/2, 1/2, 1/2)$, and zero in all corner points of $Q = (0, 1)^3$. In this case, we have $\overline{u} \in X \cap H^{3/2-\varepsilon}(Q)$, $\varepsilon > 0$, and we observe 1.5 as the order of convergence, see Table 2, which corresponds to the error estimate (3.17).

As a third example (Example 4.1.3), we take a piecewise constant discontinuous target $\overline{u}$ which is one in the inscribed cube $(\frac{1}{4}, \frac{3}{4})^3$, and zero elsewhere. In this case, we have $\overline{u} \in H^{1/2-\varepsilon}(Q)$, $\varepsilon > 0$. From the numerical results given in Table 3, we observe 0.5 for the order of convergence, as expected from the error estimate (3.12). In this example, since the target $\overline{u}$ is discontinuous, we may apply an adaptive refinement based on the residual type error indicator as used in [20]. We compare the errors and number of degrees of freedom using both uniform and adaptive refinements in Table 4, with respect to the regularization parameter ϱ. We clearly see that for each regularization parameter ϱ, the adaptive refinement requires less degrees of freedom to reach a similar accuracy as for uniform refinements. In Fig. 1, we plot the state $\widetilde{u}_{\varrho h}$, the adjoint state $\widetilde{p}_{\varrho h}$, and the control $\widetilde{z}_{\varrho h}$ at time $t = 0.5$, and the adaptive meshes in space-time. For comparison of the results with different regularization terms, we refer to the numerical results in [20]. From this, we can conclude that adaptivity is especially important when the target is discontinuous in space and time. Using space-time adaptivity, we can achieve the same accuracy with a much smaller number of degrees of freedom.

The next example (Example 4.1.4) is taken from [21] with the target given by the non-tensor-product function

$$\overline{u} = \left(1.0 + \exp\left(\frac{\cos(g(t))\left(\frac{70}{3} - 70x_1\right) + \sin(g(t))\left(\frac{70}{3} - 70x_2\right)}{\sqrt{2}}\right)\right)^{-1} + \left(1.0 + \exp\left(\frac{\cos(g(t))\left(70x_1 - \frac{140}{3}\right) + \sin(g(t))\left(70x_2 - \frac{140}{3}\right)}{\sqrt{2}}\right)\right)^{-1} - 1$$

Table 1 Error $\|\widetilde{u}_{\varrho h} - \overline{u}\|_{L^2(Q)}$ in the case of a smooth target $\overline{u}$ given by (4.3) (Example 4.1.1)

h	$\varrho\ (= h^2)$	$\|\widetilde{u}_{\varrho h} - \overline{u}\|_{L^2(Q)}$	eoc
2^{-2}	2^{-4}	2.2380e−1	
2^{-3}	2^{-6}	9.0449e−2	1.31
2^{-4}	2^{-8}	2.6491e−2	1.77
2^{-5}	2^{-10}	6.9335e−3	1.93
2^{-6}	2^{-12}	1.7613e−3	1.98
2^{-7}	2^{-14}	4.4352e−4	1.99
2^{-8}	2^{-16}	1.0600e−4	2.06
2^{-9}	2^{-18}	2.6836e−5	1.98

Table 2 Error $\|\widetilde{u}_{\varrho h} - \overline{u}\|_{L^2(Q)}$ in the case of a piecewise linear continuous target $\overline{u} \in X \cap H^{3/2-\varepsilon}(Q)$, $\varepsilon > 0$ (Example 4.1.2)

h	$\varrho\ (= h^2)$	$\|\widetilde{u}_{\varrho h} - \overline{u}\|_{L^2(Q)}$	eoc
2^{-2}	2^{-4}	2.0231e−1	
2^{-3}	2^{-6}	9.1319e−2	1.15
2^{-4}	2^{-8}	3.4303e−2	1.41
2^{-5}	2^{-10}	1.2428e−2	1.46
2^{-6}	2^{-12}	4.4443e−3	1.48
2^{-7}	2^{-14}	1.5797e−3	1.49
2^{-8}	2^{-16}	5.5868e−4	1.50
2^{-9}	2^{-18}	1.9786e−4	1.50

Table 3 Error $\|\widetilde{u}_{\varrho h} - \overline{u}\|_{L^2(Q)}$ in the case of a discontinuous target $\overline{u} \in H^{1/2-\varepsilon}(Q)$, $\varepsilon > 0$ (Example 4.1.3)

h	$\varrho\ (= h^2)$	$\|\widetilde{u}_{\varrho h} - \overline{u}\|_{L^2(Q)}$	eoc
2^{-2}	2^{-4}	2.8840e−1	
2^{-3}	2^{-6}	2.0871e−1	0.47
2^{-4}	2^{-8}	1.4793e−1	0.50
2^{-5}	2^{-10}	1.0473e−1	0.50
2^{-6}	2^{-12}	7.4108e−2	0.50
2^{-7}	2^{-14}	5.2425e−2	0.50
2^{-8}	2^{-16}	3.7079e−2	0.50
2^{-9}	2^{-18}	2.6219e−2	0.50

Table 4 Comparison of the error $\|\widetilde{u}_{\varrho h} - \overline{u}\|_{L^2(Q)}$ and the number of degrees of freedoms in the case of a discontinuous target $\overline{u} \in H^{1/2-\varepsilon}(Q)$, $\varepsilon > 0$, when using both uniform and adaptive refinements (Example 4.1.3)

	Uniform refinement			Adaptive refinement	
ϱ	$h = \varrho^{1/2}$	#DOFs	$\|\widetilde{u}_{\varrho h} - \overline{u}\|_{L^2(Q)}$	#DOFs	$\|\widetilde{u}_{\varrho h} - \overline{u}\|_{L^2(Q)}$
2^{-4}	2^{-2}	250	2.8840e−1	250	2.8840e−1
2^{-6}	2^{-3}	1, 458	2.0871e−1	1, 230	2.0873e−1
2^{-8}	2^{-4}	9, 826	1.4793e−1	9, 948	1.3999e−1
2^{-10}	2^{-5}	71, 874	1.0473e−1	34, 998	1.0153e−1
2^{-12}	2^{-6}	549, 250	7.4108e−2	230, 154	7.2804e−2
2^{-14}	2^{-7}	4, 293, 378	5.2425e−2	1, 526, 400	5.1838e−2
2^{-16}	2^{-8}	33, 949, 186	3.7079e−2	6, 196, 200	3.6609e−2
2^{-18}	2^{-9}	270, 011, 394	2.6219e−2	31, 419, 720	2.5824e−2

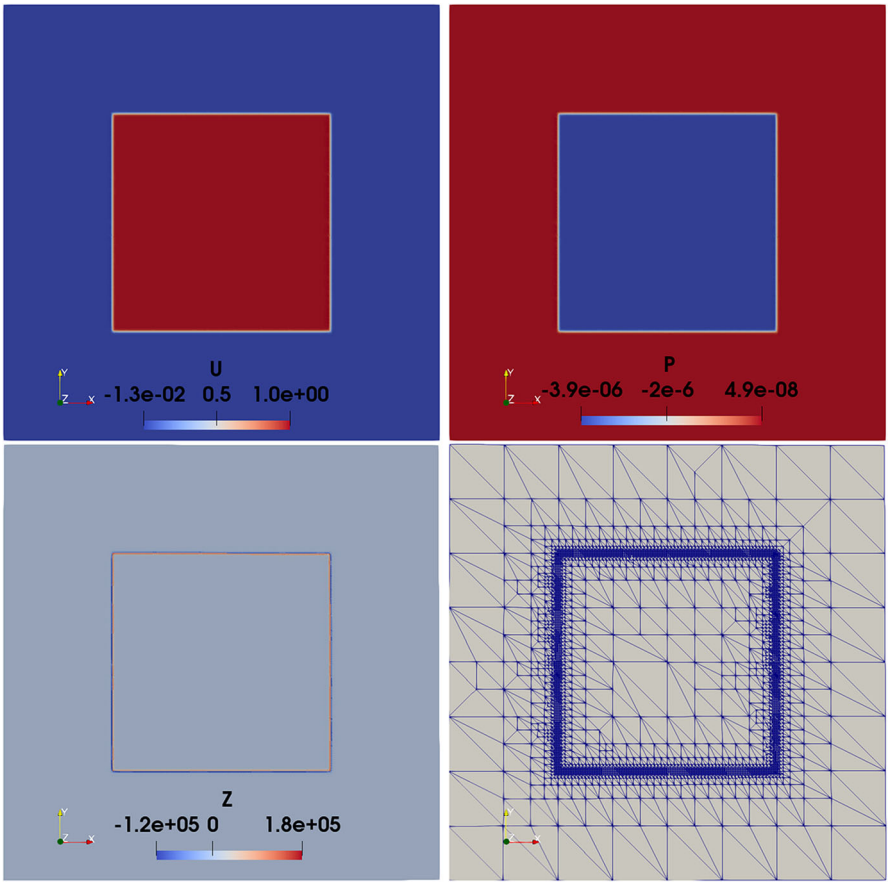

Fig. 1 Visualization of the state $\widetilde{u}_{\varrho h}$, the adjoint state $\widetilde{p}_{\varrho h}$, the control $\widetilde{z}_{\varrho h}$, and the adaptive mesh on the cutting plane at time $t = 0.5$, where the total #DOFs in space-time is 3, 328, 617 at the 58th adaptive level from 67 levels (last line in Table 4) corresponding to the regularization parameter $\varrho = 2^{-18}$ (Example 4.1.3)

in $Q = (0, 1)^3$, where $g(t) = \frac{2\pi}{3} \min\left\{\frac{3}{4}, t\right\}$. This target has the form of a turning wave, and was originally considered in [9]. It is easy to see that this target does not fulfill homogeneous boundary and initial conditions. The comparison of uniform and adaptive refinements are illustrated in Tables 5 and 6, where we have used the adaptive versions with a global constant regularization parameter $\varrho = h_{\min}^2$ and locally varying regularization parameters $\varrho_\tau = h_\tau^2$ for every finite element τ from the mesh $\mathcal{T}_h$, respectively. Both lead to a considerable reduction in number of degrees of freedom to reach similar accuracy as in the case of the uniform refinement. The adaptive refinement shows much better convergence than the uniform one. We mention that, for the optimal control of elliptic equations, the varying regularization has been studied in [18]. The analysis of varying regularization for parabolic optimal control problems will be presented in another work. We have here used the simple error indicator $\|\overline{u} - \widetilde{u}_{\varrho h}\|_{L^2(\tau)}$ for driving the adaptivity. In fact, $\|\overline{u} - \widetilde{u}_{\varrho h}\|^2_{L^2(Q)} = \sum_\tau \|\overline{u} - \widetilde{u}_{\varrho h}\|^2_{L^2(\tau)}$ is considered to be an a posteriori error estimator. This is indeed even an exact error representation.

Table 5 Comparison of the error $\|\widetilde{u}_{\varrho h} - \overline{u}\|_{L^2(Q)}$ and the number of degrees of freedoms in the case of the turning wave target $\overline{u} \in H^{1/2-\varepsilon}(Q)$, $\varepsilon > 0$, when using both uniform and adaptive refinements (Example 4.1.4)

Uniform refinement					Adaptive refinement	
ϱ	$h = \varrho^{1/2}$	#DOFs	$\|\widetilde{u}_{\varrho h} - \overline{u}\|_{L^2(Q)}$	eoc	#DOFs	$\|\widetilde{u}_{\varrho h} - \overline{u}\|_{L^2(Q)}$
2^{-4}	2^{-2}	250	4.8768e−1	–	250	4.8768e−1
2^{-6}	2^{-3}	1, 458	3.3923e−1	0.52	1, 448	2.4784e−1
2^{-8}	2^{-4}	9, 826	2.1894e−1	0.63	6, 316	1.5861e−1
2^{-10}	2^{-5}	71, 874	1.4087e−1	0.64	21, 646	1.0699e−1
2^{-12}	2^{-6}	549, 250	9.4223e−2	0.58	32, 942	8.0533e−2
2^{-14}	2^{-7}	4, 293, 378	6.5418e−2	0.53	117, 568	5.6716e−2
2^{-16}	2^{-8}	33, 949, 186	4.6082e−2	0.51	1, 202, 496	3.6361e−2
2^{-18}	2^{-9}	270, 011, 394	3.2565e−2	0.50	1, 868, 602	2.7711e−2

In the adaptive refinement, we have used $\varrho = h^2_{\min}$ over all tetrahedral elements

The computed state $\widetilde{u}_{\varrho h}$, adjoint state $\widetilde{p}_{\varrho h}$, and the corresponding control $\widetilde{z}_{\varrho h}$ at time $t = 0.5$ are illustrated in Fig. 2. We also observe that the local refinements are concentrated on that part of the boundary where the target does not fulfill the homogeneous Dirichlet condition, and the interface inside the domain. From this example, we can also confirm that adaptivity plays an important role when the target is rotating in time or does not fulfill homogeneous initial and boundary conditions. Similar accuracy is obtained with much fewer degrees of freedom using space-time adaptivity in comparison with uniform refinement.

In the last example (Example 4.1.5) of this subsection, we consider the discontinuous target

$$\overline{u}^{\delta} = \overline{u} + 2\sqrt{2}\delta \sin(10\pi x_1) \sin(10\pi x_2) \sin(10\pi t), \tag{4.4}$$

Table 6 Comparison of the error $\|\widetilde{u}_{\varrho h} - \overline{u}\|_{L^2(Q)}$ and the number of degrees of freedoms in the case of the turning wave target $\overline{u} \in H^{1/2-\varepsilon}(Q)$, $\varepsilon > 0$, when using both uniform and adaptive refinements (Example 4.1.4)

Uniform refinement					Adaptive refinement	
ϱ	$h = \varrho^{1/2}$	#DOFs	$\|\widetilde{u}_{\varrho h} - \overline{u}\|_{L^2(Q)}$	eoc	#DOFs	$\|\widetilde{u}_{\varrho h} - \overline{u}\|_{L^2(Q)}$
2^{-4}	2^{-2}	250	4.8768e−1	–	250	4.8768e−1
2^{-6}	2^{-3}	1, 458	3.3923e−1	0.52	1, 954	2.7931e−1
2^{-8}	2^{-4}	9, 826	2.1894e−1	0.63	9, 286	1.8121e−1
2^{-10}	2^{-5}	71, 874	1.4087e−1	0.64	32, 540	1.3209e−1
2^{-12}	2^{-6}	549, 250	9.4223e−2	0.58	98, 348	8.9221e−2
2^{-14}	2^{-7}	4, 293, 378	6.5418e−2	0.53	442, 082	5.6638e−2
2^{-16}	2^{-8}	33, 949, 186	4.6082e−2	0.51	1, 276, 384	4.2062e−2
2^{-18}	2^{-9}	270, 011, 394	3.2565e−2	0.50	4, 410, 618	2.9702e−2

In the adaptive refinement, we have used variable $\varrho_\tau = h^2_\tau$ on each tetrahedral element

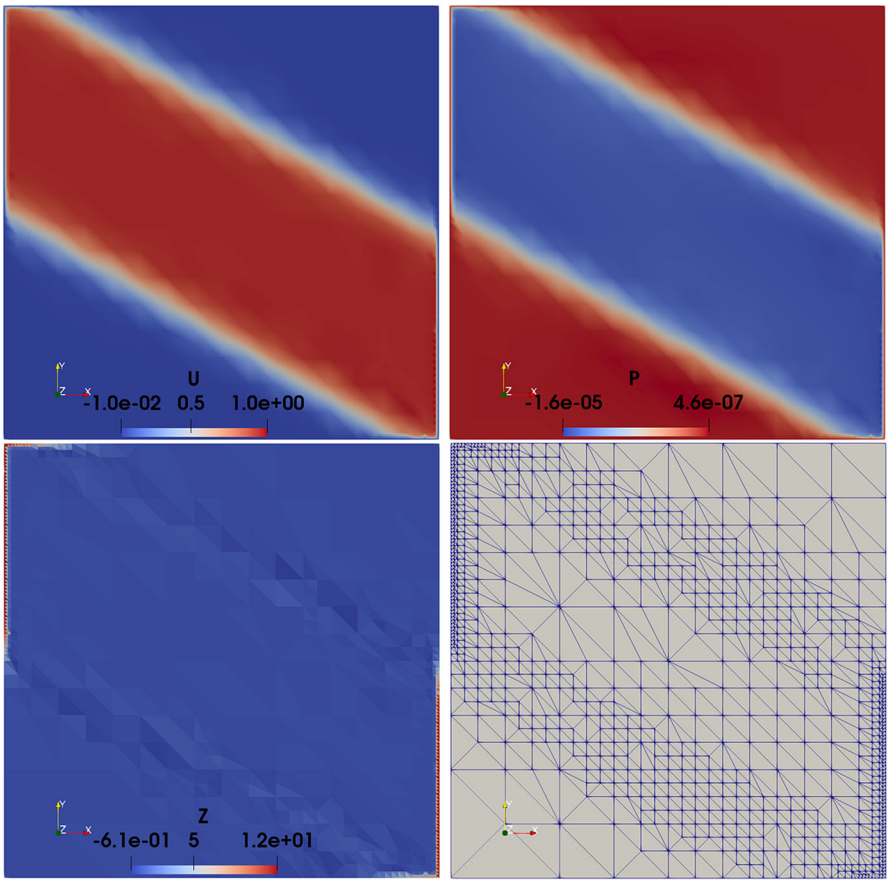

Fig. 2 Visualization of the state $\widetilde{u}_{\varrho h}$, the adjoint state $\widetilde{p}_{\varrho h}$, the control $\widetilde{z}_{\varrho h}$, and the adaptive mesh on the cutting plane at time $t = 0.5$, where the total #DOFs in space-time is 117, 568 at the 17th adaptive level (see the sixth row in Table 5) corresponding to the regularization parameter $h^2_{\min}$ (Example 4.1.4)

that contains some noise in space and time. Here, $\overline{u}$ is one in the inscribed cube $(1/4, 3/4)^3 \subset (0, 1)^3$ and zero else, cf. Example 4.1.3, and $\delta > 0$ is the noise level. For this polluted target, we easily see that $\|\overline{u}^\delta - \overline{u}\|_{L^2(Q)} = \delta$. To balance the two error contributions we take $h = 16\,\delta^2$. This ensures an almost optimal convergence with respect to the mesh size h, see Table 7.

4.2 Three space dimensions

Now we present some numerical results for the three-dimensional spatial domain $\Omega = (0, 1)^3$, i.e., $Q = (0, 1)^4$.

In the first example (Example 4.2.1), we look at the smooth target

$$\overline{u}(x, t) = \sin(\pi x_1) \sin(\pi x_2) \sin(\pi x_3) \sin(\pi t). \tag{4.5}$$

Table 7 Error $\|\widetilde{u}^{\delta}_{\varrho h} - \overline{u}\|_{L^2(Q)}$ in the case of a discontinuous target $\overline{u} \in H^{1/2-\varepsilon}(Q)$ containing some noise level δ (Example 4.1.5)

δ	$h\ \left(=16\cdot\delta^2\right)$	$\varrho\ \left(=h^2\right)$	$\|\widetilde{u}^{\delta}_{\varrho h} - \overline{u}\|_{L^2(Q)}$	eoc
2^{-3}	2^{-2}	2^{-4}	2.8841e−1	
$2^{-3.5}$	2^{-3}	2^{-6}	2.0871e−1	0.47
2^{-4}	2^{-4}	2^{-8}	1.4796e−1	0.50
$2^{-4.5}$	2^{-5}	2^{-10}	1.0535e−1	0.49
2^{-5}	2^{-6}	2^{-12}	7.6837e−2	0.46
$2^{-5.5}$	2^{-7}	2^{-14}	5.5990e−2	0.46

As predicted by the error estimate (3.14), we observe a second-order convergence with respect to the mesh size h when choosing $\varrho = h^2$; see Table 8 and Fig. 3.

In the second example (Example 4.2.2), we take a piecewise linear continuous target function $\overline{u}$ being one in the midpoint $(1/2, 1/2, 1/2, 1/2)$ and zero in all corner points of $Q = (0, 1)^4$. In this case we have $\overline{u} \in X \cap H^{3/2-\varepsilon}$, $\varepsilon > 0$, and we observe 1.5 as order of convergence which corresponds to the error estimate (3.17), see Table 9 and Fig. 4.

In the third example (Example 4.2.3), we consider a piecewise constant discontinuous target $\overline{u}$ which is one in the inscribed cube $(\frac{1}{4}, \frac{3}{4})^4$, and zero else. In this case we have $\overline{u} \in H^{1/2-\varepsilon}(Q)$, $\varepsilon > 0$. From the numerical results as given in Table 10 we observe 0.5 for the order of convergence, as expected from the error estimate (3.12), see also Fig. 5.

4.3 Solver studies

We are now going to provide some first performance studies for the solvers that we used to solve the corresponding systems of finite element equations. We solely present numerical results for the turning wave example (Example 4.1.4) that is certainly the most involved benchmark considered in this paper.

Table 8 Error $\|\widetilde{u}_{\varrho h} - \overline{u}\|_{L^2(Q)}$ in the case of the smooth target $\overline{u}$ given by (4.5) (Example 4.2.1)

N(#DOFs)	$h = (N/2)^{-1/4}$	$\varrho\ (= h^2)$	$\|\widetilde{u}_{\varrho h} - \overline{u}\|_{L^2(Q)}$
356	2.7378e−1	7.4953e−2	2.0985e−1
630	2.3737e−1	5.6344e−2	1.7263e−1
2, 986	1.6087e−1	2.5880e−2	1.2166e−1
6, 930	1.3034e−1	1.6988e−2	9.3733e−2
38, 114	8.5111e−2	7.2439e−3	4.7198e−2
94, 146	6.7890e−2	4.6091e−3	3.2098e−2
546, 562	4.3737e−2	1.9129e−3	1.4088e−2
1, 400, 322	3.4570e−2	1.1951e−3	8.8652e−3
8, 289, 026	2.2163e−2	4.9121e−4	3.7164e−3
21, 657, 090	1.7432e−2	3.0389e−4	2.2967e−3
129, 165, 826	1.1155e−2	1.2444e−4	9.5061e−4

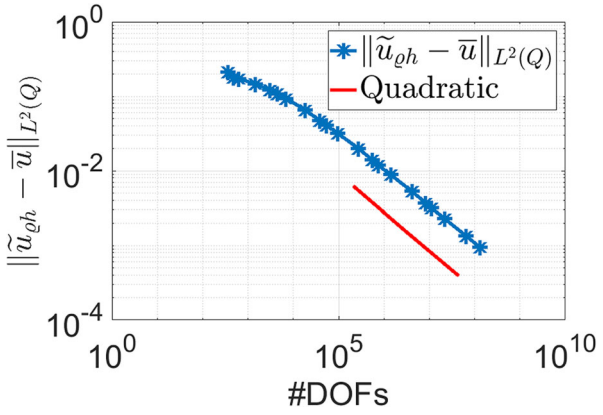

Fig. 3 Error $\|\widetilde{u}_{\varrho h} - \overline{u}\|_{L^2(Q)}$ in the case of a smooth desired state $\overline{u} \in H_0^1(Q) \cap H^2(Q)$ in three space dimensions (Example 4.2.1)

We first look at the number of iterations (#GMRES Its) needed by the ILU(0) preconditioned GMRES method for solving the coupled system (4.1) in the case of both uniform and adaptive refinements; see Table 11. We observe growing iteration numbers with decreasing mesh size, as expected. However, the growth of the iteration numbers is moderate. So, the simple ILU(0) preconditioned GMRES solver can be used for solving small and midsize systems.

To solve large-scale systems efficiently, the use of asymptotically optimal solvers is inescapable. Surprisingly, for the optimal choice $\varrho = h^2$ of the regularization parameter, we observe that the Schur complement $S_h = \varrho B_h^\top A_h^{-1} B_h + M_h$ is spectrally equivalent to the mass matrix M_h and, therefore, to some diagonal replacement like the lumped mass matrix $\mathrm{lump}(M_h)$. More precisely, we can prove the spectral equivalent inequalities

$$\frac{1}{n+2}\,\mathrm{lump}(M_h) \le M_h \le S_h \le (c+1)\,M_h \le (c+1)\,\mathrm{lump}(M_h), \tag{4.6}$$

Table 9 Error $\|\widetilde{u}_{\varrho h} - \overline{u}\|_{L^2(Q)}$ in the case of a piecewise linear continuous target $\overline{u} \in X \cap H^{3/2-\varepsilon}(Q)$, $\varepsilon > 0$ (Example 4.2.2)

N(#DOFs)	$h = (N/2)^{-1/4}$	$\varrho\ (= h^2)$	$\|\widetilde{u}_{\varrho h} - \overline{u}\|_{L^2(Q)}$
356	2.7378e−1	7.4953e−2	2.1510e−1
630	2.3737e−1	5.6344e−2	1.7972e−1
2, 986	1.6087e−1	2.5880e−2	1.3082e−1
6, 930	1.3034e−1	1.6988e−2	1.0510e−1
38, 114	8.5111e−2	7.2439e−3	6.1638e−2
94, 146	6.7890e−2	4.6091e−3	4.5864e−2
546, 562	4.3737e−2	1.9129e−3	2.4759e−2
1, 400, 322	3.4570e−2	1.1951e−3	1.7766e−2
8, 289, 026	2.2163e−2	4.9121e−4	9.2755e−3
21, 657, 090	1.7432e−2	3.0389e−4	6.5280e−3
129, 165, 826	1.1155e−2	1.2444e−4	3.3636e−3

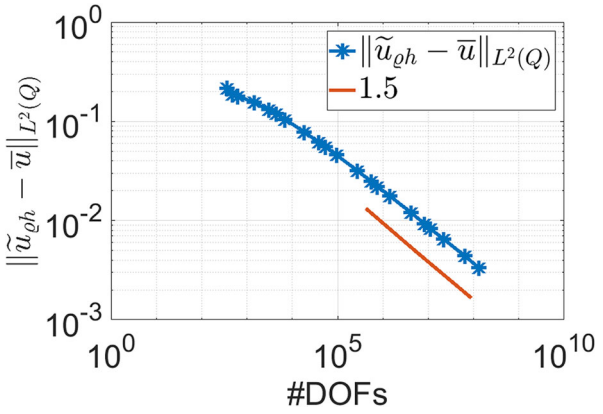

Fig. 4 Error $\|\widetilde{u}_{\varrho h} - \overline{u}\|_{L^2(Q)}$ in the case of a piecewise linear continuous target $\overline{u} \in X \cap H^{3/2-\varepsilon}(Q)$, $\varepsilon > 0$ (Example 4.2.2)

with $c = (c_F + 1)c_{\text{inv}}^2$, where the positive constants c_F and c_{inv} are defined by the spatial Friedrichs inequality (3.2) and the inverse inequality

$$\|\nabla u_h\|_{L^2(Q)} \leq c_{\text{inv}} h^{-1} \|u_h\|_{L^2(Q)}, \ \forall u_h \in X_h, \tag{4.7}$$

respectively. Indeed, for all nodal vectors $\underline{u} \in \mathbb{R}^{M_X}$, we have the estimates

$$\begin{aligned}(\varrho B_h^\top A_h^{-1} B_h \underline{u}, \underline{u}) &= \varrho \sup_{\underline{q} \in \mathbb{R}^{M_Y}} \frac{(B_h \underline{u}, \underline{q})^2}{(A_h \underline{q}, \underline{q})} \\ &= \varrho \sup_{q_h \in Y_h} \frac{\left[\int_0^T \int_\Omega [\, \partial_t u_h \, q_h + \nabla_x u_h \cdot \nabla_x q_h \,] \, dx \, dt \right]^2}{\int_0^T \int_\Omega \nabla_x q_h \cdot \nabla_x q_h \, dx \, dt}\end{aligned}$$

Table 10 Error $\|\widetilde{u}_{\varrho h} - \overline{u}\|_{L^2(Q)}$ in the case of a piecewise constant and discontinuous target $\overline{u} \in H^{1/2-\varepsilon}(Q)$, $\varepsilon > 0$ (Example 4.2.3)

N(#DOFs)	$h = (N/2)^{-1/4}$	$\varrho\ (= h^2)$	$\|\widetilde{u}_{\varrho h} - \overline{u}\|_{L^2(Q)}$
356	2.7378e−1	7.4953e−2	2.5099e−1
630	2.3737e−1	5.6344e−2	1.9143e−1
2, 986	1.6087e−1	2.5880e−2	1.8823e−1
6, 930	1.3034e−1	1.6988e−2	1.7500e−1
38, 114	8.5111e−2	7.2439e−3	1.4710e−1
94, 146	6.7890e−2	4.6091e−3	1.3313e−1
546, 562	4.3737e−2	1.9129e−3	1.0558e−1
1, 400, 322	3.4570e−2	1.1951e−3	9.6592e−2
8, 289, 026	2.2163e−2	4.9121e−4	7.7744e−2
21, 657, 090	1.7432e−2	3.0389e−4	6.8891e−2
129, 165, 826	1.1155e−2	1.2444e−4	5.5284e−2

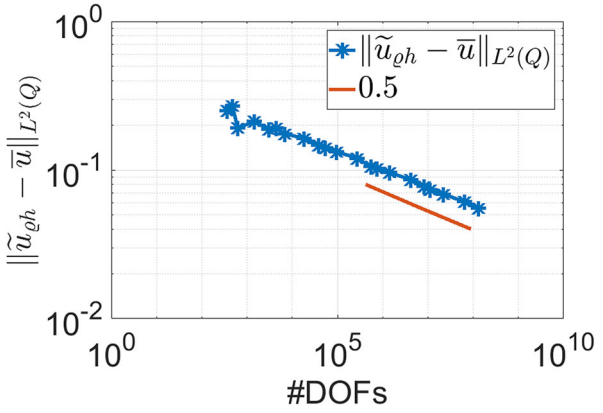

Fig. 5 Error $\|\widetilde{u}_{\varrho h} - \overline{u}\|_{L^2(Q)}$ in the case of a piecewise constant and discontinuous target $\overline{u} \in H^{1/2-\varepsilon}(Q)$, $\varepsilon > 0$ (Example 4.2.3)

$$
\begin{aligned}
&\leq \varrho \sup_{q_h \in Y_h} \frac{\|\nabla u_h\|^2_{L^2(Q)} (\|q_h\|^2_{L^2(Q)} + \|\nabla_x q_h\|^2_{L^2(Q)})}{\|\nabla_x q_h\|_{L^2(Q)}} \\
&\leq (c_F + 1)\varrho \|\nabla u_h\|^2_{L^2(Q)} \leq (c_F + 1)\varrho h^{-2} c^2_{\text{inv}} \|u_h\|^2_{L^2(Q)} \\
&\leq (c_F + 1) c^2_{\text{inv}} (M_h \underline{u}, \underline{u}),
\end{aligned}
$$

which together with the spectral equivalence inequalities

$$
(n+2)^{-1} \operatorname{lump}(M_h) \leq M_h \leq \operatorname{lump}(M_h)
$$

complete the proof of the spectral equivalence inequalities (4.6).

The spectral equivalent inequalities (4.6) immediately yield that the Schur complement system (4.2) can be solved by the Preconditioned Conjugate Gradient (PCG)

Table 11 Number of ILU(0) preconditioned GMRES method (#GR Its) for solving the coupled system (4.1) on both the uniform and adaptive refinements

Uniform (h^2)		Adaptive ($h^2_{\min}$)		Adaptive (h^2_τ)	
#DOFs	#GR Its	#DOFs	#GR Its	#DOFs	#GR Its
250	6	250	6	250	6
1, 458	15	1, 448	15	1, 954	22
9, 826	28	6, 316	24	9, 286	40
71, 874	47	21, 646	30	32, 540	72
549, 250	77	32, 942	36	98, 348	84
4, 293, 378	121	117, 568	58	442, 082	216
33, 949, 186	168	1, 202, 496	106	1, 276, 384	219
270, 011, 394	222	1, 868, 602	153	4, 410, 618	344

Here we use the 2D turning wave from (Example 4.1.4) as target

method where the lumped mass matrix lump(M_h) provides an asymptotically optimal preconditioner. This observation and the spectral equivalence of the Schur complement S_h to the mass matrix M_h imply that the PCG iterates reach a fixed relative accuracy in the M_h energy norm respectively in the $L^2(Q)$ norm within a constant number of iterations independent of the mesh size h. This theoretical result can be observed from the first column of Table 12 (uniform refinement) where the number of PCG iterations (#PCG Its) required to reduce the relative preconditioned residual error by a factor 10^7 is displayed. The same is true for the case of adaptive refinement with $\varrho = h^2_{\min}$ and $\varrho_\tau = h^2_\tau$. For simplicity, in the matrix-vector multiplication $S_h * \underline{u}^k$, the inner inversion A_h^{-1} applied to a given vector $\underline{r}$ is realized by applying the standard Ruge-Stüben Algebraic Multigrid (AMG) solver to $A_h \underline{q} = \underline{r}$ such that the relative residual error is reduced by factor 10^{10} across all meshes considered. We refer the reader to [28] for Ruge-Stüben's AMG. This accuracy can be adapted to the discretization error, and the PCG solver can be embedded in a nested iteration strategy across the discretization levels. This nested iteration procedure should be stopped if the approximation of the computed state to the desired state reaches a given accuracy or if the cost for the control exceeds some threshold. In Table 13, the nested mass-lumped PCG iterations (#NPCG), the corresponding errors $\|\widetilde{u}_{\varrho h} - \overline{u}\|_{L^2(Q)}$, and the computational time in seconds (s) on the uniform refinements are illustrated. Herein, on the coarsest level $l = 1$, we solve the linear system until the relative residual error is reduced by a factor 10^5. On the refined level $l > 1$, we stop the iteration when the relative preconditioned residual error is smaller than $\alpha[n_l/n_{l-1}]^{-\frac{\beta}{3}}$, $l = 2, 3, ...$, with $\beta = 0.5$, $\alpha = 0.5$, and n_l being the number of vertices on the level l. Herein, the inner AMG iteration stops when the relative residual error is reduced by factor 10^2 on all levels. This requires about $2-3$ AMG iterations. The solution on the coarse level is used as the initial guess for the solution on the fine level. We clearly observe that the number of PCG iterations is significantly reduced without loss of accuracy of the numerical discretization, in comparison with the errors and convergence for the uniform refinement in Tables 4 and 5, and number of PCG iterations for uniform refinement in Table 12.

Table 12 Number of PCG iterations (#PCG Its) for solving the Schur complement system (4.2) on both the uniform and adaptive refinements, using the lumped mass as the preconditioner

Uniform (h^2)		Adaptive ($h^2_{\min}$)		Adaptive (h^2_τ)	
#DOFs	#PCG Its	#DOFs	#PCG Its	#DOFs	#PCG Its
125	13	125	13	125	13
729	24	724	32	977	29
4, 913	30	3, 158	39	4, 643	34
35, 937	32	10, 823	41	16, 270	34
274, 625	32	16, 471	36	49, 174	35
2, 146, 689	31	58, 784	34	221, 041	37
16, 974, 593	30	601, 248	41	638, 192	35
135, 005, 697	29	934, 301	33	2, 205, 309	32

Here we use the 2D turning wave from (Example 4.1.4) as target

Table 13 The error $\|\widetilde{u}_{\varrho h} - \overline{u}\|_{L^2(Q)}$, the number of nested mass-lumped preconditioned PCG iterations (#NPCG), and the time in seconds in the case of the turning wave target $\overline{u} \in H^{1/2-\varepsilon}(Q)$, $\varepsilon > 0$, for the uniform refinements (Example 4.1.4)

ϱ	$h = \varrho^{1/2}$	#DOFs	$\|\widetilde{u}_{\varrho h} - \overline{u}\|_{L^2(Q)}$	eoc	#NPCG Its	Time (s)
2^{-4}	2^{-2}	125	4.8801e−1	–	22	0.01
2^{-6}	2^{-3}	729	3.3837e−1	0.53	3	0.01
2^{-8}	2^{-4}	4, 913	2.1748e−1	0.64	3	0.08
2^{-10}	2^{-5}	35, 937	1.3948e−1	0.64	3	0.79
2^{-12}	2^{-6}	274, 625	9.3125e−2	0.58	3	6.38
2^{-14}	2^{-7}	2, 146, 689	6.4684e−2	0.53	3	89.94
2^{-16}	2^{-8}	16, 974, 593	4.5587e−2	0.50	3	627.60
2^{-18}	2^{-9}	135, 005, 697	3.2221e−2	0.50	3	5, 740.41

Herein, we have used adaptive stopping threshold in the nested iterations

We mention that the inner AMG iteration within the matrix-vector multiplication can be avoided when solving the symmetric, infinite system (4.1), e.g., by the Bramble-Pasciak PCG [6].

5 Conclusions and outlook

We have derived robust space-time finite element error estimates for distributed parabolic optimal control problems with energy regularization. More precisely, we have estimated the $L^2(Q)$ norm of the error between the desired state $\overline{u}$ and the computed state $\widetilde{u}_{\varrho h}$ depending on the regularity of the desired state $\overline{u}$. It has been shown that the optimal convergence rate is achieved by the proper scaling $\varrho = h^2$ between the regularization parameter ϱ and the mesh size h. The theoretical findings are confirmed by several numerical examples in both two and three space dimensions.

The theoretical results are valid for uniform mesh refinement. However, for discontinuous targets $\overline{u}$ and targets that do not fulfill the boundary or initial conditions, we can expect layers with steep gradients in the solutions as in Examples 4.1.3, 4.1.4 and 4.2.3. In these examples, we have observed that, for a fixed $\varrho = h^2$, the adaptive version needs considerably less unknowns to achieve the same accuracy as the corresponding uniformly refined grid with the finest mesh size h. Since, for adaptively refined grids, the local mesh sizes are very different, one may also think about a localization of the regularization parameter ϱ, see [18] in the case of an elliptic distributed optimal control problem. For simplicity, we use the ILU(0) preconditioned GMRES as standard solver for the symmetric, but indefinite system (4.1). This solver is not asymptotically optimal with respect to the arithmetical complexity. The construction and investigation of fast and ϱ robust solvers for the symmetric and indefinite systems like (4.1) is still an interesting research topic in connection with optimal control problems; see, e.g., [1, 2, 25, 27, 29, 30, 37] and the references therein. For the optimal choice of $\varrho = h^2$, the first theoretical and numerical results presented in Section 4.3

show that one can construct asymptotically optimal solvers for (4.1) or even for the Schur complement system (4.2), in particular, when the solvers are embedded in a nested iteration strategy. The analysis of solvers for variable (local) choice of the regularity parameter as a function of (x, t) is another future research topic.

Finally, the consideration of constraints imposed on the control z_Q or the state u_Q is of practical interest; see, e.g., the monographs [23] and [35], and the very recent publication [12] in connection with energy regularization for elliptic distributed optimal control problems.

Acknowledgements The authors would like to acknowledge the computing support of the supercomputer MACH–2 (https://www3.risc.jku.at/projects/mach2/) from the Johannes Kepler Universität Linz and of the high performance computing cluster Radon1 (https://www.oeaw.ac.at/ricam/hpc) from the Johann Radon Institute for Computational and Applied Mathematics (RICAM) on which the numerical experiments were performed. The first and the third authors were partially supported by RICAM. Furthermore, the authors would like to express their thanks to the anonymous referees for their helpful and inspiring comments.

Funding Open access funding provided by Graz University of Technology.

Declarations

Conflict of interest The authors declare no competing interests.

References

1. Bai, Z.-Z., Benzi, M., Chen, F., Wang, Z.-Q.: Preconditioned MHSS iteration methods for a class of block two-by-two linear systems with applications to distributed control problems. IMA J. Numer. Anal. **33**(1), 343–369 (2013)
2. Benzi, M., Golub, G.H., Liesen, J.: Numerical solution of saddle point problems. Acta Numer **14**, 1–137 (2005)
3. Beranek, N., Reinhold, M.A., Urban, K.: A space-time variational method for optimal control problems: Well-posedness, stability and numerical solution. Comput. Optim. Appl. **86**, 767–794 (2023)
4. Bey, J.: Tetrahedral grid refinement. Computing **55**, 355–378 (1995)
5. Borzì, A., Schulz, V.: Computational optimization of systems governed by partial differential equations, vol. 8 of Computational Science & Engineering. SIAM, (2011)
6. Bramble, J.H., Pasciak, J.E.: A preconditioning technique for indefinite systems resulting from mixed approximations of elliptic problems. Math. Comp. **50**(181), 1–17 (1988)
7. Brenner, S., Scott, R.: The Mathematical Theory of Finite Element Methods. Texts Appl. Math. vol. 15. Springer, New York (2008)
8. Casas, E.: A review on sparse solutions in optimal control of partial differential equations. SeMA Journal **74**, 319–344 (2017)
9. Casas, E., Ryll, C., Tröltzsch, F.: Sparse optimal control of the Schlögl and FitzHugh-Nagumo systems. Comput. Methods Appl. Math. **13**(4), 415–442 (2013)
10. Ern, A., Guermond, J.-L.: Theory and Practice of Finite Elements. Springer, New York (2004)

11. Führer, T., Karkulik, M.: Space-time finite element methods for parabolic distributed optimal control problems. Comput. Methods Appl. Math., accepted, (2024)
12. Gangl, P., Löscher, R., Steinbach, O.: Regularization and finite element error estimates for elliptic distributed optimal control problems with energy regularization and state or control constraints (2023). arXiv:2306.15316
13. Gantner, G., Stevenson, R.: Applications of a space-time FOSLS formulation for parabolic PDEs. IMA J. Numer. Anal. **44**(1), 58–82 (2024)
14. Gong, W., Hinze, M., Zhou, Z.: Space-time finite element approximation of parabolic optimal control problems. J. Numer. Math. **20**(2), 111–145 (2012)
15. Gunzburger, M., Kunoth, A.: Space-time adaptive wavelet methods for optimal control problems constrained by parabolic evolution equations. SIAM J. Control. Optim. **49**(3), 1150–1170 (2011)
16. Hinze, M., Pinnau, R., Ulbrich, M., Ulbrich, S.: Optimization with PDE Constraints, vol. 23. Springer, Berlin (2009)
17. John V.: Finite Element Methods for Incompressible Flow Problems, vol. 51 of Springer Series in Computational Mathematics. Springer, (2016)
18. Langer, U., Löscher, R., Steinbach, O., Yang, H.: An adaptive finite element method for distributed elliptic optimal control problems with variable energy regularization. Comput. Math. Appl. **160**, 1–14 (2024)
19. Langer, U., Schafelner, A.: Adaptive space-time finite element methods for parabolic optimal control problems. J. Numer. Math. **30**(4), 247–266 (2022)
20. Langer, U., Steinbach, O., Tröltzsch, F., Yang, H.: Space-time finite element discretization of parabolic optimal control problems with energy regularization. SIAM J. Numer. Anal. **59**(2), 660–674 (2021)
21. Langer, U., Steinbach, O., Tröltzsch, F., Yang, H.: Unstructured space-time finite element methods for optimal control of parabolic equation. SIAM J. Sci. Comput. **43**(2), A744–A771 (2021)
22. Langer, U., Steinbach, O., Yang, H.: Robust discretization and solvers for elliptic optimal control problems with energy regularization. Comput. Meth. Appl. Math. **22**(1), 97–111 (2022)
23. Lions, J.L.: Contrôle optimal de systèmes gouvernés par des équations aux dérivées partielles. Dunod Gauthier-Villars, Paris (1968)
24. Lions, J.-L., Magenes, E.: Non-homogeneous boundary value problems and applications I. Springer, New York-Heidelberg (1972)
25. Mardal, K.-A., Winther, R.: Preconditioning discretizations of systems of partial differential equations. Numer. Linear Algebra Appl. **18**(1), 1–40 (2011)
26. Neumüller, M., Steinbach, O.: Regularization error estimates for distributed control problems in energy spaces. Math. Methods Appl. Sci. **44**, 4176–4191 (2021)
27. Pearson, J.W., Stoll, M., Wathen, A.J.: Preconditioners for state-constrained optimal control problems with Moreau-Yosida penalty function. Numer. Linear Algebra Appl. **21**(1), 81–97 (2014)
28. Ruge, J.W., Stüben, K.: Algebraic multigrid (AMG). In: McCormick, S.F. (ed.) Multigrid Methods, pp. 73–130. SIAM, Philadelphia (1987)
29. Schöberl, J., Zulehner, W.: Symmetric indefinite preconditioners for saddle point problems with applications to PDE-constrained optimization problems. SIAM J. Matrix Anal. Appl. **29**, 752–773 (2007)
30. Schulz, V., Wittum, G.: Transforming smoothers for pde constrained optimization problems. Comput. Visual. Sci. **11**(4), 207–219 (2008)
31. Steinbach, O.: Space-time finite element methods for parabolic problems. Comput. Meth. Appl. Math. **15**(4), 551–566 (2015)
32. Steinbach, O., Zank, M.: Coercive space-time finite element methods for initial boundary value problems. Electron. Trans. Numer. Anal. **52**, 154–194 (2020)
33. Stevenson, R.: The completion of locally refined simplicial partitions created by bisection. Math. Comput. **77**(261), 227–241 (2008)
34. Tartar, L.: An Introduction to Sobolev Spaces and Interpolation Spaces. Lecture Notes of the Unione Matematica Italiana, vol. 3. Springer, Berlin (2007)
35. Tröltzsch, F.: Optimal control of partial differential equations: Theory, methods and applications. Graduate Studies in Mathematics, vol. 112. American Mathematical Society, Providence, Rhode Island (2010)
36. Zeidler, E.: Nonlinear Functional Analysis and its Applications II/B: Nonlinear Monotone Operators. Springer, New York (1990)
37. Zulehner, W.: Nonstandard norms and robust estimates for saddle point problems. SIAM J. Matrix Anal. Appl. **32**(2), 536–560 (2011)